



UNIVERSITY OF LEEDS

This is a repository copy of *Intra-annual stable isotopes in the tree rings of Hymenaea courbaril as a proxy for hydroclimate variations in southern Amazonia*.

White Rose Research Online URL for this paper:

<https://eprints.whiterose.ac.uk/206311/>

Version: Accepted Version

Article:

Guimarães, K.S., Marimon, B.S., Locosselli, G.M. et al. (8 more authors) (2023) Intra-annual stable isotopes in the tree rings of *Hymenaea courbaril* as a proxy for hydroclimate variations in southern Amazonia. *Dendrochronologia*, 83. 126151. ISSN 1125-7865

<https://doi.org/10.1016/j.dendro.2023.126151>

© 2023 Published by Elsevier. This is an author produced version of an article published in *Dendrochronologia*. Uploaded in accordance with the publisher's self-archiving policy. This manuscript version is made available under the CC-BY-NC-ND 4.0 license <http://creativecommons.org/licenses/by-nc-nd/4.0/>.

Reuse

This article is distributed under the terms of the Creative Commons Attribution-NonCommercial-NoDerivs (CC BY-NC-ND) licence. This licence only allows you to download this work and share it with others as long as you credit the authors, but you can't change the article in any way or use it commercially. More information and the full terms of the licence here: <https://creativecommons.org/licenses/>

Takedown

If you consider content in White Rose Research Online to be in breach of UK law, please notify us by emailing eprints@whiterose.ac.uk including the URL of the record and the reason for the withdrawal request.



eprints@whiterose.ac.uk
<https://eprints.whiterose.ac.uk/>

1 **Intra-annual stable isotopes in the tree rings of *Hymenaea courbaril* as a proxy for**
2 **hydroclimate variations in southern Amazonia**

3 Karollyne Silva Guimarães^{a,*}, Beatriz Schwantes Marimon^a, Giuliano Maselli
4 Locosselli^b, Roel Brienen^c, Bruno Barcante Ladvoat Cintra^d, Arnoud Boom^f, Igor Araújo^a,
5 Ben Hur Marimon-Junior^a, Gregório Ceccantini^e, Wesley Jonatar A. da Cruz^a, Oliver L.
6 Phillips^c

7

8 ^aUniversidade do Estado de Mato Grosso, Programa de Pós-Graduação em
9 Ecologia e Conservação, BR 158, km 655, CEP: 78690-000, Nova Xavantina, Mato
10 Grosso, Brazil

11 ^bUniversidade de São Paulo, Centro de Energia Nuclear na Agricultura, Avenida
12 Centenário, 303, 13416-000, Piracicaba, São Paulo, Brazil

13 ^cUniversity of Leeds, School of Geography, LS2 9JT, Leeds, United Kingdom

14 ^dUniversity of Birmingham, School of Geography, Earth and Environmental
15 Sciences, B15 2TT, Birmingham, United Kingdom

16 ^eUniversidade de São Paulo, Instituto de Biociências, Departamento de Botânica,
17 Rua do Matão 277, CEP: 05508-090, São Paulo, Brazil

18 ^fUniversity of Leicester, School of Geography Geology and the Environment, LE1
19 7RH, Leicester, United Kingdom

20 *Correspondence to: Universidade do Estado de Mato Grosso, Programa de Pós-
21 Graduação em Ecologia e Conservação, BR 158, km 655, CEP: 78690-000, Nova
22 Xavantina, Mato Grosso, Brazil.

23 E-mail address: karoline.guimaraes@outlook.com (K. S. Guimarães).

24

25 E-mail addresses: karoline.guimaraes@outlook.com (K. S. Guimarães),
26 biamarimon@unemat.br (B. S. Marimon), locosselli@cena.usp.br (G. M. Locosselli),
27 r.brienen@leeds.ac.uk (R. W. Brienen), brunoblcintra@gmail.com (B. B. L. Cintra),
28 ab269@le.ac.uk (A. Boom), igor.araujo@outlook.com.br (I. Araújo),

29 bhmarimon@unemat.br (B. H. Marimon-Junior), gregorio@usp.br (G. Ceccantini),
30 wesleyjonatar@gmail.com (W. J. A. da Cruz), o.phillips@leeds.ac.uk (O. L. Phillips).

31

32 **Highlights**

- 33 1. Tree rings of *Hymenaea courbaril* show a pronounced intra-annual variation in
34 $\delta^{13}\text{C}$, and weaker variation in $\delta^{18}\text{O}$.
- 35 2. Intra-annual variation in $\delta^{13}\text{C}$ reflects carbon remobilization at the start of the
36 growing season, while intra-annual $\delta^{18}\text{O}$ variation reflects seasonal variation in
37 precipitation- $\delta^{18}\text{O}$ and climate.
- 38 3. Year to year variation in tree ring $\delta^{18}\text{O}$ is correlated with variation in regional river
39 discharge and offers a good potential for seasonal climate reconstructions.

40

41 **Abstract**

42 The hydrology of Amazonia is changing due to climate and land-use changes,
43 especially in the southern region, which has warmed and dried faster than other tropical
44 regions. Yet there are no long-term hydrological records to put these changes in a
45 historical perspective. Here we investigate the use of tree-ring carbon ($\delta^{13}\text{C}$) and oxygen
46 isotopes ($\delta^{18}\text{O}$) to assess the seasonal variation in climate for the southern Amazonia
47 basin. We analysed the intra-annual variation of $\delta^{13}\text{C}$ and $\delta^{18}\text{O}$ in 10 segments for each
48 tree ring from 2013 to 2017 from individuals of *Hymenaea courbaril*, a long-lived and
49 widespread neotropical tree species. We find strong seasonal patterns of tree-ring $\delta^{13}\text{C}$
50 supporting previous observations of annual growth rhythms for this species. The intra-
51 annual variation in $\delta^{18}\text{O}$ shows point to the lowest values generally just after the middle
52 of the rings that corresponds to the peak rainy season. We find strong correlations
53 between the $\delta^{18}\text{O}$ in the middle of the growth ring and vapour pressure deficit ($r =$
54 0.92 , $P = 0.02$) and precipitation ($r = -0.93$, $P = 0.02$). We further find associations
55 between the oxygen isotopic series and the discharge of the Araguaia basin's main rivers
56 during the rainy period. Our results show that these $\delta^{18}\text{O}$ records are sensitive to
57 fluctuations in rainfall and humidity, and thus reflect river discharge in the region, and that
58 longer reconstructions of $\delta^{18}\text{O}$ tree ring of *Hymenaea courbaril* could provide a novel
59 proxy to assess past hydrological changes.

60

61 Keywords: jatobá-da-mata, oxygen isotopes, carbon isotopes, intra-annual
62 isotopes, river discharge.

63

64 **Introduction**

65 Observations suggest that climate change and land-use change have resulted in
66 increased amplitude of the hydrological cycle across the Amazonia, affecting the length
67 of the dry period and the frequency of rainfall extremes during the wet season (Fu et al.,
68 2013; Gloor et al., 2013; Barichivich et al., 2018; Espinoza et al., 2019). Climate models
69 suggest these changes in precipitation regime may become more extreme in coming
70 years (Nobre et al., 2009; Boisier et al., 2015; Alves et al., 2017). For instance, the historic
71 drought of 2015-2016 serves as an example of this trend (Jiménez-Muñoz et al., 2016),
72 which is likely to affect river discharge (Callède et al., 2004; Cavalcante et al., 2019;
73 Heerspink et al., 2020) as well as tree growth, mortality, and other key aspects of forest
74 dynamics (Aleixo et al., 2019; Esquivel-Muelbert et al., 2020; Reis et al., 2022). Most river
75 discharge observations rely on long-term hydrological records from central Amazonia that
76 go back as far as 1902 for the Rio Amazonas and 1903 for the Rio Negro (Richey et al.,
77 1989; Espinoza et al., 2022). In contrast, reliable records in southern Amazonia tend to
78 be more recent, dating back only to 1971 (Coe et al., 2011; Ho et al., 2016). This region,
79 however, has seen an increase in deforestation (Gatti et al., 2021), experienced the
80 highest rates of warming, and is drying faster than anywhere else in the basin (Malhi et
81 al., 2008; Jiménez-Muñoz et al., 2013; Haghtalab et al., 2020) or indeed any other tropical
82 site (Jiménez-Muñoz et al., 2013; Alves et al., 2017; IPCC, 2022). While climate change
83 threatens to disrupt ecosystems and societies in these rapidly changing regions, we lack
84 good, long-term climate records essential for understanding climate impacts. Thus,
85 alternative proxies are urgently needed to help put these recent changes in a long-term
86 perspective.

87 Pre-instrumental climate can be assessed through natural archives like tree-ring
88 widths and stable isotopes (McCarroll and Loader, 2004). In the tropics, tree-ring stable
89 oxygen isotope ($\delta^{18}\text{O}$) variation has been shown to reflect primarily the isotopic
90 composition of source water (i.e., precipitation, Brienen et al., 2012, 2013; Baker et al.,
91 2015, 2016). The main processes that affect this source water (or precipitation) $\delta^{18}\text{O}$ in

92 the tropics are the rainout of heavy isotopes during transport to the site of condensation
93 and the local precipitation processes (Dansgaard, 1964; Vuille and Werner, 2005). The
94 first of these, the rainout of heavier water (H_2O^{18}) during water vapour transport trajectory
95 is affected by the accumulated rainfall along the water vapour transport to the site of
96 condensation (Vuille and Werner 2005). Longer travel distances and lower temperatures
97 and higher precipitation will result in lower (more depleted) $\delta^{18}\text{O}$ values. On top of this,
98 local precipitation intensity - often referred to as the “amount effect” - additionally affects
99 precipitation. Usually in the tropics, there is an inverse relationship between the amount
100 of precipitation and the $\delta^{18}\text{O}$ (Dansgaard, 1964; Risi et al. 2008). In inland sites in the
101 Amazonia basin, the isotopic composition of precipitation is inversely related to the
102 amount of precipitation during water transport from the Atlantic Ocean to the site of
103 precipitation (Salati et al., 1979; Vuille et al., 2003). This is because water vapour gets
104 gradually depleted in heavy isotopes (H_2O^{18}) due to Rayleigh rainout processes leading
105 to lower $\delta^{18}\text{O}$ during years with heavy precipitation (Dansgaard, 1964; Vuille and Werner,
106 2005; Risi et al., 2008). Tree-ring $\delta^{18}\text{O}$ in humid sites in the Amazonia basin strongly
107 reflects this variation in precipitation $\delta^{18}\text{O}$, with relatively minor influences of leaf water
108 enrichment (Brienen et al., 2012; Cintra et al., 2019). These previous results also show
109 that tree-ring $\delta^{18}\text{O}$ in the western parts of the Amazonia basin primarily reflect the large-
110 scale rainout processes (i.e., rainout during water vapour transport over land; Brienen et
111 al., 2012; Baker et al., 2016).

112 While oxygen isotopes can thus be used to reconstruct large-scale variation in
113 precipitation, additional analysis of carbon isotopes ($\delta^{13}\text{C}$) in tree rings may provide
114 insights into plant physiological responses to climate (Barbour et al., 2004; Kahmen et
115 al., 2011; Cintra et al., 2019). The $\delta^{13}\text{C}$ is a measure of the discrimination against ^{13}C
116 during CO_2 diffusion into the leaf and subsequent fractionation during carboxylation
117 (photosynthesis). Greater stomatal limitation over photosynthesis (i.e. during dry
118 conditions when stomata tend to close) results in lower discrimination and consequently
119 higher $\delta^{13}\text{C}$ values, while wetter conditions result in lower $\delta^{13}\text{C}$ (Farquhar et al., 1982;
120 Barbour et al., 2000). At an intra-annual scale, carbon isotope variation between early
121 wood and late wood is additionally affected by the remobilization of stored carbon
122 reserves for annual wood production (Gessler et al., 2014; Locosselli et al., 2020).

123 Long-term trends in hydroclimate are usually assessed through tree-ring isotopes
124 on an inter-annual basis (e.g., ring by ring; Danis et al., 2006; Li et al., 2020; Pagotto et

125 al., 2021). However, high-resolution, intra-ring analysis can provide a useful lens into
126 details of the seasonal climate variability during the growing season when using oxygen
127 isotopes (Li et al., 2011; Monson et al., 2018), or in the case of carbon isotopes, provide
128 insights in the seasonality of wood formation and use of carbohydrates (Cintra et al.,
129 2019; Locosselli et al., 2020). This can be done by dividing tree rings into sub-annual
130 segments that are then separately analysed in terms of isotopic composition. This
131 approach has been used for assessing intra-annual variation of precipitation (Managave
132 et al., 2010; Schubert and Timmermann, 2015; Muangsong et al., 2020; Xu et al., 2020),
133 to study the hydrological cycle (Alvarez et al., 2018) and to assess a metropolitan area
134 water supply (Locosselli et al., 2020). We here test this intra-annual approach to provide
135 insight into seasonal $\delta^{18}\text{O}$ and $\delta^{13}\text{C}$ patterns and test its potential for reconstruction of
136 past climate variation.

137 We aim to evaluate the strength of the climate signal in the rings of trees from the
138 southern fringes of the Amazonia, a global hotspot of warming and an ecologically
139 critically climate-sensitive location. We analysed high-resolution stable isotopes in tree
140 rings of *Hymenaea courbaril* L., (locally denominated jatobá-da-mata), a long-lived,
141 widespread neotropical species that can exceed 300 years old (Locosselli et al., 2017).
142 Although *H. courbaril* tree rings have been proven annual (Lucchi, 1998; Westbrook et
143 al., 2006; Lisi et al., 2008) and widely used before (e.g., Locosselli et al., 2013, 2016),
144 some recent carbon dating studies cast doubt on the annual nature of its rings under
145 seemingly less seasonal climate conditions (Santos et al., 2021). We analysed carbon
146 and oxygen stable isotopes in ten segments of each tree ring produced between 2013
147 and 2017 (two years prior to and two years following the drought of 2016) to address the
148 following questions: 1) Is intra-annual variation in $\delta^{13}\text{C}$ and $\delta^{18}\text{O}$ for
149 *H. courbaril* consistent with expected patterns due to tree physiology and seasonal
150 variation in climate?; 2) Can oxygen isotopic signals be used to reconstruct seasonal flow
151 of the main rivers in the region during the wet season?

152

153 **Materials and methods**

154

155 *2.1. Study area and Species*

156 Sampling took place in a large fragment of forest located in the legal reserve area
157 of Fazenda Vera Cruz (14°49'32"S and 52°06'20"W), Nova Xavantina, Mato Grosso,
158 Brazil (Fig. 1). It is located at the transition of Amazonia and *Cerrado* biomes (Ratter et
159 al., 1973; Marimon et al., 2014; Marques et al., 2020), and considered a pre-Amazonian
160 transitional forest (Mews et al., 2012; Marimon et al., 2014). It is a closed canopy forest
161 with trees that can reach 25 m in height (Marimon et al., 2006, 2014; Mews et al., 2012).
162 The forest fragment lies in the Araguaia River Basin which is more than 2,300 km long,
163 has a drainage area of approximately 380,000 km², and its main tributary is the das
164 Mortes River with length of 1,070 km and a drainage area of about 62,000 km² (Fig. 1;
165 Latrubesse and Stevaux, 2002; Rosin et al., 2015).

166 The climate is seasonal Aw type according to the Köppen classification (Alvares et
167 al., 2013), with an average annual precipitation of 1369 mm, and two well-defined
168 seasons, a rainy from October to March and a dry season that lasts six months when
169 monthly rainfall is lower than 50 mm month⁻¹ (April to September, Fig. 2). The middle of
170 the dry season corresponds to the hottest months of the year when maximum air
171 temperatures regularly exceed 40 °C (Tiwari et al., 2020; Araújo et al., 2021).

172 We sampled trees of *H. courbaril*, a brevi-deciduous species that gradually replaces
173 all old leaves with new ones during the dry season, but rarely becomes completely
174 leafless (Lisi et al., 2008). It is characterised by a cylindrical trunk and it reaches heights
175 of up to 35 metres tall, often emerging above the forest canopy (Carvalho, 2003). The
176 tree rings of *H. courbaril* are visually distinct and delimited by a marginal parenchyma
177 band (Locosselli et al., 2013). Although its growth rings have previously been proven to
178 be annual (Luchi, 1998; Westbrook, 2006), recent studies using radiocarbon dating raised
179 doubts about their annual nature (e.g., Santos et al., 2021).

180 We collected 39 increment cores from 17 living *H. courbaril* trees between March
181 and July 2018 using a gasoline-powered Stihl drill with a borer of 1.5 cm in diameter and
182 1 m in length coupled to a motor drill (Krottenthaler et al., 2015). We collected three to
183 four perpendicular radii from each tree, at breast height, or approximately 1.3 m from the
184 topsoil. After sample collection, we closed the holes in the tree trunks with natural cork
185 (Locosselli et al., 2016). Data on tree diameter at breast height (DBH), height, overall
186 conditions, presence of lianas, and geographical coordinates were recorded for each tree
187 in the field.

188

189 *2.2. Sample preparation and tree-ring analysis*

190 We glued the increment cores on wooden supports and, after drying them at room
191 temperature for a couple of weeks, we polished them using sandpaper with different grits
192 (60, 120, 220, 300, 400, 600, 1200, and 2000). After polishing, we scanned the samples
193 with the EPSON Expression 12000XL Scanner and analysed the images using the
194 WinDendro software (Regent Instruments) to identify, count, and measure the width of
195 the tree rings. We visually cross-dated the tree rings among the radii of the same
196 individual and then between the radii of different individuals, looking for the pointer years
197 that correspond to narrow rings common to most trees in a population (Schweingruber et
198 al., 1990). From the sampled specimens were included in the chronology 17 trees with
199 between 1 and 3 radii with clearly visible and demarcated rings (Fig. A1, Table A1).

200

201 *2.3. Tree-ring isotope analyses*

202 For isotopic analysis, we chose rings from the period from 2013 to 2017 to capture
203 the 2015–2016 El Niño year, which was the hottest year recorded in recent times (Bennett
204 et al., *in press*). The preparation of isotopic samples was done at the University of Leeds.
205 We choose three trees with wide and distinct tree rings for the intra-annual isotope
206 analysis (Fig. A2). We used a circular saw (Proxxon KS 230, Saw Blade 28 020,
207 Locosselli et al., 2020) to cut transversal thin sections with a thickness of 2mm from the
208 increment cores, and then isolated full segments from the thin sections containing the
209 years from 2013 to 2017. These thin wood sections were then placed inside supports
210 made from Teflon sheets to extract cellulose as per Kagawa et al. (2015). We treated the
211 samples twice in a 5% NaOH solution for 2 hours in a water bath at 60 °C to remove
212 resins, fatty acids, and tannins. We then washed the samples with deionized boiling water
213 and treated the samples four times in 7.5% NaClO₂ solution at pH 4-5, also in a water
214 bath at 60 °C, totaling 37 hours. We finally washed the samples with deionized boiling
215 water and dried them in a lyophilizer (Kagawa et al., 2015; Schollaen et al., 2015).

216 To assess the intra-annual isotope patterns, we sampled 10 segments from each
217 ring, totalizing 300 samples. Ring sections were separated according to weight rather
218 than width which avoids problems with variation in growth rate throughout the growing

219 season between trees and has been shown to result in a strong common signal observed
 220 among specimens (Locosselli et al., 2020). To do this, we first cut out a sample of
 221 cellulose of the entire tree ring equalling 10 times the target weight for stable isotope
 222 analyses (i.e. 10 * 0.5 mg for $\delta^{18}\text{O}$ + 10 * 1 mg for $\delta^{13}\text{C}$ = 15 mg). We then removed thin
 223 sections of cellulose, layer by layer, measuring their weight using a precision scale until
 224 it reached the total weight of 1.5 mg. This procedure was performed for each of the ten
 225 segments within a ring (and until all cellulose was used up). We packed 0.5 mg in silver
 226 cups for oxygen isotopes and we packed 1 mg of cellulose in tin cups for carbon isotopes
 227 analysis.

228 The isotope analysis was done at the University of Leicester. Oxygen isotope ratios
 229 were then measured using an Isotopes Ratio Monitoring Mass Spectrometer (Sercon 20-
 230 20 IRMS, Sercon IRMS, Crewe-UK) interfaced to a high temperature furnace, equipped
 231 with a glassy carbon reactor at 1400 degrees C°. Laboratory cellulose standards were
 232 measured after every 10 samples and these were used to calculate the precision
 233 (precision = 0.15‰). Carbon isotopes were separately measured over an elemental
 234 analyzer coupled to the same mass spectrometer and precision was determined using
 235 cellulose laboratory standards (precision = 0.1‰). Isotopic ratios were expressed
 236 according to the delta notation. The isotopic ratios for the pure cellulose standards
 237 (sigma-aldrich) were $\delta^{13}\text{C} = -24.9\text{‰}$ and $\delta^{18}\text{O} = 29.8\text{‰}$.

$$\delta = \left[\frac{\left[\frac{^{13}\text{C}}{^{12}\text{C}} \right]_{\text{sample}}}{\left[\frac{^{13}\text{C}}{^{12}\text{C}} \right]_{\text{standard}}} - 1 \right] \times 1000$$

238

239

240 *2.4. Intra-annual isotope series synchronisation*

241 For each year, we synchronised the isotope series among different trees by shifting
 242 the entire individual $\delta^{18}\text{O}$ series one or two positions to the left or right (see example Fig.
 243 A3) to match the valleys and picks of all series in a year. This procedure aims at correcting
 244 eventual temporal offsets in the start and end of the growth season, or differences in the
 245 rate of cambial growth rate during the growing season among individuals (see Locosselli

246 et al., 2020). We only shifted the full intra-annual series and did not merge the values of
247 adjacent intra-annual positions, nor did we split any series for synchronisation.

248 The decision on the best relative position of the individual series was taken based
249 on the calculated Gleichläufigkeit (GLK) values that is a measure of the common signal
250 between series (Eckstein and Bauch, 1969). The GLK is a nonparametric method used
251 in dendrochronology to evaluate the strength of the synchronization by calculating the
252 percent common year-to-year growth changes between two tree ring series. For each
253 year in which the growth rate of the series is in phase, in other words similarly increases
254 or decreases in two tree-ring series, a value equal to one is summed, while if growth is in
255 anti-phase, a value minus one is summed. In cases when one series changes the growth
256 rate in a year and the other one remains constant, a value equal to zero is attributed. The
257 average of these values allows one to assess the synchrony between the two analysed
258 series, and how this synchrony changes when shifting the inter-annual series for the best
259 dating position. We used the same principle here, but instead of looking for changes in
260 the inter-annual variation of tree-ring width, we sought for the synchrony between intra-
261 annual $\delta^{18}\text{O}$ values for each year between 2013 and 2017. We performed a pairwise
262 comparison of the intra-annual series for each year, and averaged the calculated GLK
263 values to choose the one that represented the best synchrony among the three series
264 (Gleichläufigkeit, Bura and Wilmking, 2015; 'dpiR', Bunn, 2008). The synchronisation
265 resulted in substantial improvements in the GLK values for all years when compared to
266 non-synchronized series, indicating a better match between the series' peaks and dips
267 (Fig. 3). The non-synchronized series of oxygen and carbon presented a mean GLK of
268 0.51 and 0.63, respectively, while the synchronised series resulted in a GLK mean of 0.68
269 for both isotopes, which represents up to a 33% increase in GLK values. We then
270 produced for both oxygen and carbon isotopes average series using the adjusted
271 (synchronised) data (Fig. 3).

272

273 *2.5. Hydroclimate correlation analysis*

274 We calculated Pearson's correlation values between the average intra-annual
275 oxygen isotopes of each tree-ring position (from one to ten) and monthly values of local
276 precipitation, vapour pressure deficit (VPD), and river discharge of the main basins of the
277 Mortes and Araguaia Rivers, and presented the result as heatmaps. We obtained local

278 precipitation and evapotranspiration data from a weather station of the National Institute
279 of Meteorology (INMET - www.inmet.gov.br, XAVANTINA - 83319) located in Nova
280 Xavantina (14°69'79" S and 52°35'02" W), about 20 km from the sampling site, and river
281 stage data from weather stations of the Brazilian National Water Resources Information
282 System (SNIRH - www.snirh.gov.br/hidroweb). The average $\delta^{18}\text{O}$ series were then
283 plotted against the climate data guided by using the intra-annual position and month with
284 the highest correlation value for visual comparison.

285 We also performed Pearson's correlation between annual isotope values and
286 annual climate data. For this, we chose the positions of oxygen isotopes within the tree
287 ring that best correlated with monthly climate data (positions 3 to 7). We averaged these
288 positions, resulting in annual values of oxygen isotopes between 2013 and 2017. Next,
289 we performed Pearson correlations between annual isotopic values and mean values of
290 local precipitation, VPD, and river discharges during the rainy season (October to March).

291

292 **Results**

293

294 *3.1. Variation in $\delta^{13}\text{C}$*

295 The intra-annual series of $\delta^{13}\text{C}$ shows a clear pattern with high values at the
296 beginning of the ring, followed by consistent decreases to minimum values towards the
297 end of the tree rings (Fig. 4). These patterns show sharp shifts in carbon isotopes values
298 near the parenchyma bands that occur in the ring boundaries between years. Specifically,
299 at the start of each tree ring, the average carbon isotope value for the individuals is
300 approximately -26‰ VSMOW, while towards the end of the tree ring the values decline
301 to approximately -27‰ VSMOW, indicating a carbon isotope shift within the ring from
302 earlywood to latewood. We did not find significant correlations between the synchronized
303 intra-annual mean $\delta^{13}\text{C}$ series and the climate data during the growing season (Fig. A3)

304

305 *3.2. Variation in $\delta^{18}\text{O}$ and hydrological records correlation*

306 The series of $\delta^{18}\text{O}$ presented a clear repeating pattern with lowest $\delta^{18}\text{O}$ values right
307 after the middle of the ring and highest values usually at the tree rings borders (Fig. 4).

308 The synchronized mean intra-annual series for $\delta^{18}\text{O}$ showed a negative correlation with
309 precipitation in January at position 5 ($r = -0.93$, $P = 0.02$; Fig. 5), and a positive correlation
310 with VPD during the month of February at position 4 ($r = 0.92$, $P = 0.02$; Fig. 5). We found
311 significant correlations between tree-ring $\delta^{18}\text{O}$ and river discharge from the two main
312 rivers of the Araguaia basin (Fig. 5). We further observed a negative correlation between
313 the $\delta^{18}\text{O}$ at positions 3 and 7 within the tree ring and Mortes streamflow of December (r
314 $= -0.93$, $P = 0.01$) and January ($r = -0.93$, $P = 0.02$; Fig. 5), respectively. The same $\delta^{18}\text{O}$
315 positions within the tree ring were also correlated with the Araguaia streamflow of
316 December ($r = -0.96$, $P = 0.04$) and January ($r = -0.93$, $P = 0.006$; Fig. 5). We also find
317 that the annual $\delta^{18}\text{O}$ series show good correlations with average climate data during the
318 rainy period, from October to March (Fig 6; Table A2). $\delta^{18}\text{O}$ is positively related to VPD (r
319 $= 0.71$, $P = 0.17$), and negatively with precipitation ($r = -0.90$, $P = 0.03$), and with river
320 flow for das Mortes ($r = -0.74$, $P = 0.14$), and Araguaia rivers ($r = -0.75$, $P = 0.13$; Fig. 6).
321 For visual comparison, according with the highest Pearson correlations, we plotted their
322 position 5 with January VPD and precipitation series. We also plotted position 5 with das
323 Mortes and the Araguaia river flow of February. The alignment between oxygen and rivers
324 series was placed in the following month (February) as we took into account the GAP
325 between the beginning of the rainy season and the rise in the river's streamflow (Marengo,
326 1995).

327

328 **Discussion**

329

330 *Evidence of annual ring formation from intra-annual isotopes*

331 *Hymenaea courbaril* has previously been used for several dendrochronological
332 studies (e.g., Locosselli et al., 2013, 2016; Andrade et al., 2019), but a recent study
333 questioned the annual nature of this species' tree rings in the Southwestern Amazonia
334 where the dry season is very short (Santos et al., 2021). In the highly seasonal
335 hydroclimate of the Southeastern Amazonia, the common intra-annual patterns of $\delta^{13}\text{C}$
336 observed in all trees and all years gives additional support to the previous observations
337 of annual rings in *H. courbaril* under seasonal sites (e.g., Westbrook et al., 2006;
338 Locosselli et al., 2016). The annual nature of these tree rings is further supported by
339 observed strong associations between intra-annual $\delta^{18}\text{O}$ and the hydroclimate in the

340 study site. For other sites, there is mixed evidence regarding the formation of annual rings
341 by this species. Annual ring formation has been found in a few cases (e.g., Westbrook et
342 al., 2006; Locosselli et al., 2016), but others also find that annual ring dating may be
343 unreliable due to the frequent occurrence of rings that are missing locally (i.e., wedging
344 ring), or across the full cross-section (i.e., years with no growth, Santos et al., 2021).
345 Though the exact reason for the occurrence of such missing rings is still unknown, it is
346 possible that it may occur more frequently at sites where climate seasonality is less
347 pronounced and subject to erratic weather fluctuations (Santos et al., 2021). It is thus
348 possible that this species may form false rings, or missing rings in regions with more
349 erratic climate seasonality, but still present annual rings at locations with under
350 pronounced climate seasonality (e.g., Westbrook et al., 2006; Locosselli et al., 2016; this
351 study). This would indeed result in wide variation in the reliability of annual ring dating in
352 *H. courbaril*, which has a widespread distribution in the Amazon covering a large range
353 of climates, including less seasonal climates (Steege et al., 2013).

354

355 *Synchronisation of isotope series*

356 The comparison of the intra-annual isotope series indicated that growth rhythms
357 were not 100% synchronised between trees. This issue became clear from the
358 mismatches between peaks and valleys in the intra-annual $\delta^{18}\text{O}$ and $\delta^{13}\text{C}$ series among
359 individuals (Fig. 3), probably due to differences between trees in the timing of onset of
360 cambium activity at the beginning of the rainy season and cambium dormancy at the end
361 of the rainy season. As illustrated in the example we used to demonstrate synchronisation
362 for the rings of 2013 (Fig. A4), trees varied in the position of peak $\delta^{18}\text{O}$ or $\delta^{13}\text{C}$. For
363 example, in 2013 peak $\delta^{18}\text{O}$ and $\delta^{13}\text{C}$ occurred in one tree at position 6 and in the other
364 two trees at later positions 7 and 8. These differences are likely due to variations in the
365 start of the cambial activity. Aligning the highest isotope values of each specimen to the
366 same position helped to correct for these temporal offsets yielding better average GLK
367 results (Fig. 3). These differences in cambium activity, as observed in our study, are
368 expected in the tropics where low phenological synchrony has been widely reported (e.g.,
369 Vogado et al., 2016; Vasconcellos et al., 2017) mostly because of inter tree differences
370 in microclimate conditions and genetic variability within the population (De Micco et al.,
371 2016; Jiménez-Noriega et al., 2021). The fact that these series could be synchronised

372 indicates that *H. courbaril* tree rings are highly sensitive to seasonal fluctuations in climate
373 conditions.

374

375 *Intra-annual variation in carbon isotopes*

376 The recurring pattern of decreasing $\delta^{13}\text{C}$ from the beginning to the end of the tree
377 ring (Fig. 3 and 4) is consistent with the expected pattern of tree ring $\delta^{13}\text{C}$ observed in
378 other temperate (Helle and Schleser, 2004; Cernusak et al., 2009; Eglin et al., 2010) and
379 tropical deciduous species (Poussart et al., 2004; Fichtler et al., 2010; Cintra et al., 2019).
380 In the initial stage of the growing season, deciduous trees depend on stored reserves of
381 starch produced during the previous growing season to support leaf flush and woody
382 growth. As starch is enriched in ^{13}C (higher $\delta^{13}\text{C}$) relative to sugars produced during
383 photosynthesis, the early part of the tree rings will have a high $\delta^{13}\text{C}$ (Eglin et al., 2010).
384 As the growing season proceeds, more and more assimilates from current photosynthesis
385 are used, resulting in a gradual decrease of wood $\delta^{13}\text{C}$ towards the end of the rings. This
386 framework has been proposed as the basic expected mechanism behind the effect of the
387 metabolism of stored reserves on $\delta^{13}\text{C}$ of wood (Helle and Schleser, 2004), with possible
388 variations from different uses of stored reserves from year to year (Eglin et al., 2010). The
389 fractionation effects associated with the use of stored carbohydrate reserves are
390 consistent with the intra-annual patterns of other tropical ring-forming species (Cintra et
391 al., 2019; Locosselli et al., 2020). The consistency of this pattern across each analysed
392 ring in this study provides support for previous observations that those rings are likely of
393 annual nature. The large influence of carbon remobilization effects that have been
394 observed in the intra-annual carbon isotope series may explain the absence of correlation
395 we observed between $\delta^{13}\text{C}$ and climate variables, and the absence of reflection in
396 seasonal hydrology. Despite we found a correlation specifically between the Rio das
397 Mortes riverflow in January and February and the isotope series, it's important to note
398 that these series don't reflect in the river level when observed at seasonal basis.

399

400 *Intra-annual variation in oxygen isotopes*

401 We observed that the middle of the tree ring has a negative association with local
402 precipitation during January, the middle of the rainy season (Fig. 6), and with precipitation

403 across a larger region covering the Southern fringes of the Amazonia Forest (Fig. A5).
404 We noted the lowest oxygen isotope values in the ring correspond to the year 2015, which
405 coincided with a historic drought recorded in the Amazon region (Fig. 5 and 6; Jiménez-
406 Muñoz et al., 2016). Other studies in the Amazonia similarly report a negative relationship
407 between $\delta^{18}\text{O}$ and regional precipitation because of the combined effects of rainout of
408 heavy isotopes during moisture transport over long distances and the amount effect
409 (Brienen et al., 2012; Baker et al., 2016; Cintra et al., 2021). Water vapour in the air that
410 reaches the study region is transported from the Atlantic Ocean by the trade winds (Fig.
411 A6), and slowly gets depleted in H_2O^{18} because of rainout of heavy water during
412 precipitation events along the trajectory (Brienen et al., 2012; Baker et al., 2016). This
413 results in the observed negative correlation between $\delta^{18}\text{O}$ and the amount of precipitation
414 in the region upstream of the sampling site (Fig. A5).

415 While the correlation between the $\delta^{18}\text{O}$ and precipitation amounts indicates an
416 influence of source water $\delta^{18}\text{O}$, we also find indications of an effect of evaporative leaf
417 water enrichment, as revealed by the positive correlation between $\delta^{18}\text{O}$ and local VPD
418 (Fig. 5). These results are in line with experiments that show that leaf water enrichment
419 is greater under low relative humidity, or under high evaporative demand (Barbour et al.,
420 2000; Roden et al., 2000; Liu et al., 2017). Field studies on leaf and wood cellulose $\delta^{18}\text{O}$
421 have shown varying effects of VPD, with strong effects of VPD on $\delta^{18}\text{O}$ under warm and/or
422 dry environmental conditions (Kahmen et al., 2011; Cintra et al., 2019) and weaker or no
423 effects in wetter sites (Anchukaitis and Evans, 2010; Brienen et al., 2012; Cintra et al.,
424 2019). Thus, the relative effects of source water influences versus leaf water in tree rings
425 may vary due to differences in leaf water enrichment due to variations in air relative
426 humidity and species' leaf-level responses (Barbour et al., 2004; Cernusak et al., 2016).
427 The relatively strong temperature increases in this region over recent years (Jiménez-
428 Muñoz et al., 2013; Alves et al., 2017; IPCC, 2022) will lead to a decrease in the relative
429 humidity of the atmosphere (Tiwari et al., 2020; Araújo et al., 2021), and may result in a
430 stronger imprint of leaf transpiration on *H. courbaril* tree-ring $\delta^{18}\text{O}$.

431 Guided by the positions and months of highest correlations with precipitation and
432 VPD, we plotted the $\delta^{18}\text{O}$ values against the continuous climate series (Fig. 5). This
433 approach aimed to visualize the relationship between tree ring oxygen isotope series and
434 the climate data more clearly. Both precipitation and evapotranspiration define river
435 basins' hydrology and river discharge (Coe et al., 2016, 2017; Maeda et al., 2017;

436 Heerspink et al., 2020). This is probably why the isotopic series of *H. courbaril* showed a
437 better association with seasonal variation of the two main rivers of the Araguaia basin
438 than with seasonal precipitation and/or VPD alone when compared at seasonal
439 perspective (Fig. 5). This association was only clear after a small temporal shift in the
440 river flow series taking into account the observed lag between the beginning of the rainy
441 period and its effects on the streamflow (Marengo, 1995). Even though it is possible to
442 observe associations between the isotopes and the monthly streamflow for both rivers,
443 the signal recorded in the tree rings of *H. courbaril* is substantially higher for the Araguaia
444 River, 150 km downstream of the sampling site than with the das Mortes River, 20 km
445 from the sampling site. Such a large-scale hydrological signal in tree-ring $\delta^{18}\text{O}$ has been
446 demonstrated before (Dinis et al., 2019), including in the Amazonia basin (Brienen et al.,
447 2012; Cintra et al., 2022), but only a few studies addressed this issue at a sub-annual
448 scale (Locosselli et al., 2020) and this is the first one in Southern Amazonia.

449

450 Potential for climate reconstructions

451 We found largely similar results when we analysed the data at an inter-annual scale.
452 This analysis showed good correlations between averaged $\delta^{18}\text{O}$ from the middle of the
453 tree ring of *H. courbaril* and precipitation, VPD, and river discharge (Fig. 6). These
454 correlations are substantially greater for the rainy season averages from October-March
455 than when compared to the whole year hydroclimatic averages (Table A2), demonstrating
456 once again that this species indeed reflects the climate and hydrology of the southern
457 portion of Amazonia during the rainy season. One caveat of our study is the short time
458 span of the analyses that could potentially lead to artificial correlations. The interannual
459 $\delta^{18}\text{O}$ data do however fit remarkably well with four different climate datasets (Fig. 6) and
460 are in the right direction of theoretical expectations and in line with several recent oxygen
461 isotope studies in the Amazon basin (Brienen et al., 2012; Baker et al., 2016; Cintra et
462 al., 2021). These findings show that oxygen stable isotopes hold great promise to
463 reconstruct / investigate hydrological rainfall and / or river discharge records at seasonal
464 and annual variation, and improve our understanding of recent climatic changes in the
465 Amazon basin. We hope that our study thus provides an incentive for the development of
466 more tree ring studies from this region, leading to long, robust hydroclimate proxies for
467 the southern Amazon.

468

469

470 **Conclusion**

471 Our results demonstrate that in regions with a well-defined dry season, *H. courbaril*
472 presents tree rings that correspond to a hydrological year. The intra-annual variation in
473 tree-ring $\delta^{18}\text{O}$ of *H. courbaril* presents a large-scale signal that can be used as a proxy
474 for assessing seasonal river discharge and annual precipitation. It is thus a potential tool
475 to reconstruct past high-frequency climate variability for a region that is experiencing
476 strong warming in recent decades. Our results indicate that $\delta^{18}\text{O}$ tree ring records at sub-
477 annual or annual resolution can provide an important proxy to understand how climate
478 changes are affecting the basin's hydrological cycle at the southern border of the
479 Amazonia. Given the constraints imposed by our limited dataset, we underscore the
480 exploratory aspect and advocate for further investigation to solidify and expand upon our
481 findings.

482

483 **Acknowledgment**

484 This study was financed by the 2017-2019 British Council Newton Fund Institutional
485 Links + CNPq Brazil PELD, also for the Coordenação de Aperfeiçoamento de Pessoal de
486 Nível Superior – Brazil (CAPES) – Finance Code 001. We thank the Conselho Nacional
487 de Desenvolvimento Científico e Tecnológico/Projetos Ecológicos de Longa Duração -
488 CNPq/PELD (Nr. 401279/2014-6 and 441244/2016-5) for financial support. O.L. Phillips
489 was supported by an ERC Advanced Grant (Tropical Forests in the Changing Earth
490 System) and a Royal Society Wolfson Research Merit Award. GML also thanks FAPESP
491 (2017/50085-3, 2019/08783-0; 2020/09251-0). RJWB was supported by NERC seedcorn
492 grant (NE/S008659/1) and NERC standard grant (NE/K01353X/1). We thank Programa
493 de Pós-Graduação em Ecologia e Conservação, Universidade do Estado de Mato Grosso
494 – UNEMAT. The authors also thank the team of the Plant Ecology Laboratory of Nova
495 Xavantina, for their assistance in data collection and for their friendship.

496

497 **References**

498 Aleixo, I., Norris, D., Hemerik, L., Barbosa, A., Prata, E., Costa, F., Poorter, L., 2019.
499 Amazonian rainforest tree mortality driven by climate and functional traits. *Nature Climate*
500 *Change* 9(5), 384-388. <https://doi.org/10.1038/s41558-019-0458-0>.

501 Alvares, C.A., Stape, J.L., Sentelhas, P.C., Gonçalves, J.D.M., Sparovek, G., 2013.
502 Köppen's climate classification map for Brazil. *Meteorologische zeitschrift* 22(6), 711-
503 728. <https://doi.org/10.1127/0941-2948/2013/0507>.

504 Alvarez, C., Bégin, C., Savard, M.M., Dinis, L., Marion, J., Smirnov, A., Bégin, Y.,
505 2018. Relevance of using whole-ring stable isotopes of black spruce trees in the
506 perspective of climate reconstruction. *Dendrochronologia* 50, 64-
507 69. <https://doi.org/10.1016/j.dendro.2018.05.004>.

508 Alves, L.M., Marengo, J.A., Fu, R., Bombardi, R.J., 2017. Sensitivity of Amazon
509 regional climate to deforestation. *American Journal of Climate Change* 6, 75-
510 98. <https://doi.org/10.4236/ajcc.2017.61005>.

511 Anchukaitis, K.J., Evans, M.N., 2010. Tropical cloud forest climate variability and
512 the demise of the Monteverde golden toad. *Proceedings of the National Academy of*
513 *Sciences* 107(11), 5036-5040. <https://doi.org/10.1073/pnas.0908572107>.

514 Andrade, V.H.F., do Amaral Machado, S., Figueiredo Filho, A., Botosso, P.C.,
515 Miranda, B.P., Schöngart, J., 2019. Growth models for two commercial tree species in
516 upland forests of the Southern Brazilian Amazon. *Forest Ecology and Management* 438,
517 215-223. <https://doi.org/10.1016/j.foreco.2019.02.030>.

518 Araújo, I., Marimon, B.S., Scalon, M.C., Fauset, S., Junior, B.H.M., Tiwari, R.,
519 Galbraith, D.R., Gloor, M.U., 2021. Trees at the Amazonia-Cerrado transition are
520 approaching high-temperature thresholds. *Environmental Research Letters* 16(3),
521 034047. <https://doi.org/10.1088/1748-9326/abe3b9>.

522 Baker, J.C.A., Hunt, S.F.P., Clerici, S.J., Newton, R.J., Bottrell, S.H., Leng, M.J.,
523 Heaton, T.H.E., Helle, G., Argollo, J., Gloor, M., Brienen, R.L.W., 2015. Oxygen isotopes
524 in tree rings show good coherence between species and sites in Bolivia. *Global Planet*
525 *Change* 133, 298–308. <https://doi.org/10.1016/j.gloplacha.2015.09.008>.

526 Baker, J.C.A., Gloor, M., Spracklen, D.V., Arnold, S.R., Tindall, J.C., Clerici, S.J.,
527 Leng, M.J., Brienen, R.J.W., 2016. What drives interannual variation in tree ring oxygen

528 isotopes in the Amazon? *Geophys Res Lett* 43, 11831–
529 11840. <https://doi.org/10.1002/2016GL071507>.

530 Barbour, M.M., Farquhar, G.D., 2000. Relative humidity-and ABA-induced variation
531 in carbon and oxygen isotope ratios of cotton leaves. *Plant, Cell & Environment* 23, 473-
532 485. <https://doi.org/10.1046/j.1365-3040.2000.00575.x>.

533 Barbour, M. M., Roden, J.S., Farquhar, G.D., Ehleringer, J.R., 2004. Expressing leaf
534 water and cellulose oxygen isotope ratios as enrichment above source water reveals
535 evidence of a Péclet effect. *Oecologia* 138, 426-435. <https://doi.org/10.1007/s00442-003-1449-3>.

537 Barichivich, J., Gloor, E., Peylin, P., Brienen, R.J.W., Schongart, J., Espinoza, J.C.,
538 Pattnayak, K.C., 2018. Recent intensification of Amazon flooding extremes driven by
539 strengthened Walker circulation. *Science advances* 4 (9),
540 eaat8785. <https://doi.org/10.1126/sciadv.aat8785>.

541 Bennett, et al., Impact of the 2015–2016 El Niño on the carbon dynamics of South
542 American tropical forests, *Nature Climate Change*, *IN PRESS*.

543 Brienen, R.J.W., Helle, G., Pons, T.L., Guyot, J., Gloor, M., 2012. Oxygen isotopes
544 in the tree rings a good proxy for Amazon precipitation and El Niño-Southern Oscillation
545 variability. *Proceedings of the National Academy of Sciences* 109, 16957-
546 16962. <https://doi.org/10.1073/pnas.1205977109>.

547 Brienen, R.J.W., Hietz, P., Wanek, W., Gloor, M., 2013. Oxygen isotopes in tree
548 rings record variation in precipitation $\delta^{18}\text{O}$ and amount effects in the south Mexico.
549 *Journal of Geophysical Research: Biogeosciences* 118, 1-
550 12. <https://doi.org/10.1002/2013JG002304>.

551 Boisier, J.P., Ciais, P., Ducharne, A., Guimberteau, M., 2015. Projected
552 strengthening of Amazonian dry season by constrained climate model simulations.
553 *Nature Climate Change* 5, 656-650. <https://doi.org/10.1038/nclimate2658>.

554 Bunn, A.G., 2008. A dendrochronology program library in R (dplR).
555 *Dendrochronologia* 26, 115-124. <https://doi.org/10.1016/j.dendro.2008.01.002>.

556 Bura, A., Wilmking, M., 2015. Correcting the calculation of the Gleichläufigkeit.
557 *Dendrochronologia* 34, 29-30. <https://doi.org/10.1016/j.dendro.2015.03.003>.

558 Callède, J., Guyot, J.L., Ronchail, J., L'Hote, Y., de Oliveira, H.N.E., 2004. Evolution
559 du debit de l'Amazone a Obidos de 1903 a 1999 / Evolution of the River Amazon's
560 discharge at Obidos from 1903 to 1999. *Hydrol Sci J* 49, 85–
561 97. <https://doi.org/10.1623/hysj.49.1.85.53992>.

562 Carvalho, P.E.R., 2003. *Espécies Arbóreas Brasileiras*. v. 1. Brasília, Embrapa
563 Informação Tecnológica. Colombo/PR: Embrapa Florestas.

564 Cavalcante, R.B.L., Pontes, P.R.M., Souza-Filho, P.W.M., Souza, E.B., 2019.
565 Opposite effects of climate and land use changes on the annual water balance in the
566 Amazon arc of deforestation. *Water Resources Research* 55(4), 3092–
567 3106. <https://doi.org/10.1029/2019WR025083>.

568 Cernusak, L.A., Tcherkez, G., Keitel, C., Cornwell, W.K., Santiago, L.S., Knoch, A.,
569 Barbour, M.M., Williams, D.G., Reich, P.B., Ellsworth, D.S., Dawson, T.E., Griffiths, H.G.,
570 2009. Why are non-photosynthetic tissues generally ¹³C enriched compared with leaves
571 in C³ plants? Review and synthesis of current hypotheses. *Functional Plant Biology* 36(3),
572 199-213. <https://doi.org/10.1071/FP08216>.

573 Cernusak, L.A., Barbour, M.M., Arndt, S.K., Cheesman, A.W., English, N.B., Feild,
574 T. S..., Farquhar, G.D. 2016. Stable isotopes in leaf water of terrestrial plants. *Plant, Cell
575 & Environment* 39(5), 1087-1102. <https://doi.org/10.1111/pce.12703>.

576 Cintra, B.B.L., Gloor, M., Boom, A., Schöngart, J., Locosselli, G.M., Brienen, R.,
577 2019. Contrasting controls on tree ring isotope variation for Amazon floodplain and terra
578 firme trees. *Tree Physiology* 39(5), 845-860. <https://doi.org/10.1093/treephys/tpz009>.

579 Cintra, B.B.L., Gloor, M., Boom, A., Schöngart, J., Baker, J.C., Cruz, F.W., Clerici,
580 S., Brienen, R.J. 2021. Tree-ring oxygen isotopes record a decrease in Amazon dry
581 season rainfall over the past 40 years. *Climate Dynamics* 59, 1401–1414.
582 <https://doi.org/10.1007/s00382-021-06046-7>.

583 Coe, M.T., Latrubesse, E.M., Ferreira, M.E., Amsler, M.L., 2011. The effects of
584 deforestation and climate variability on the streamflow of the Araguaia River, Brazil.
585 *Biogeochemistry* 105(1), 119-131. <https://doi.org/10.1007/s10533-011-9582-2>.

586 Coe, M.T., Macedo, M.N., Brando, P.M., Lefebvre, P., Panday, P., Silvério, D., 2016.
587 The hydrology and energy balance of the Amazon basin. Interactions between biosphere,

588 atmosphere and human land use in the Amazon basin 35-53. <https://doi.org/10.1007/978->
589 3-662-49902-3_3.

590 Coe, M.T., Brando, P.M., Deegan, L.A., Macedo, M.N., Neill, C., Silvério, D.V., 2017.
591 The forests of the Amazon and Cerrado moderate regional climate and are the key to the
592 future. *Tropical Conservation Science* 10,
593 1940082917720671. <https://doi.org/10.1177/1940082917720671>.

594 Danis, P.A., Masson-Delmotte, V., Stievenard, M., Guillemin, M.T., Daux, V.,
595 Naveau, P., Von Grafenstein, U., 2006. Reconstruction of past precipitation $\delta^{18}\text{O}$ using
596 tree-ring cellulose $\delta^{18}\text{O}$ and $\delta^{13}\text{C}$: A calibration study near Lac d'Annecy, France. *Earth*
597 and *Planetary Science Letters* 243(3-4), 439-
598 448. <https://doi.org/10.1016/j.epsl.2006.01.023>.

599 Dansgaard, W., 1964. Stable isotopes in precipitation. *Tellus XVI* 4, 436-
600 468. <https://doi.org/10.3402/tellusa.v16i4.8993>.

601 De Micco, V., Campelo, F., de Luis, M., Bräuning, A., Grabner, M., Battipaglia, G.,
602 Cherubini, P., 2016. Intra-annual density fluctuations in tree rings: how, when, where, and
603 why?. *IAWA Journal* 37(2), 232-259. <https://doi.org/10.1163/22941932-20160132>.

604 Dinis, L., Bégin, C., Savard, M.M., Marion, J., Brigode, P., Alvarez, C., 2019. Tree-
605 ring stable isotopes for regional discharge reconstruction in eastern Labrador and
606 teleconnection with the Arctic Oscillation. *Clim Dyn* 53, 3625-
607 3640. <https://doi.org/10.1007/s00382-019-04731-2>.

608 Eckstein, D., Bauch, J., 1969. Beitrag zur Rationalisierung eines
609 dendrochronologischen Verfahrens und zur Analyse seiner Aussagesicherheit.
610 *Forstwissenschaftliches Centralblatt* 88, 230-250.

611 Eglin, T., Francois, C., Michelot, A., Delpierre, N., Damesin, C., 2010. Linking intra-
612 seasonal variations in climate and tree-ring $\delta^{13}\text{C}$: A functional modelling approach.
613 *Ecological Modelling* 221, 1779-1787. <https://doi.org/10.1016/j.ecolmodel.2010.04.007>.

614 Espinoza, J.C., Ronchail, J., Marengo, J.A., Segura, H., 2019. Contrasting North-
615 South changes in Amazon wet-day and dry-day frequency and related atmospheric
616 features (1981-2017). *Climate Dynamics* 52, 5413-
617 5430. <https://doi.org/10.1007/s00382-018-4462-2>.

618 Espinoza, J.C., Marengo, J.A., Schongart, J., Jimenez, J.C. 2022. The new
619 historical flood of 2021 in the Amazon River compared to major floods of the 21st century:
620 atmospheric features in the context of the intensification of floods. *Weather and Climate*
621 *Extremes* 35, 100406. <https://doi.org/10.1016/j.wace.2021.100406>.

622 Farquhar, G.D., O'Leary, M.H., Berry, J.A., 1982. On the relationship between
623 carbon isotope discrimination and intercellular carbon dioxide concentration in leaves.
624 *Australian Journal of Plant Physiology* 9, 121–137. <https://doi.org/10.1071/PP9820121>.

625 Fichtler, E., Helle, G., Worbes, M., 2010. Stable-carbon isotope time series from
626 tropical tree rings indicate a precipitation signal. *Tree-ring research* 66(1), 35-49.

627 Fu, R., Yin, L., Li, W., Arias, P.A., Dickison, R.E., Huang, L., Chakraborty, S.,
628 Fernandes, K., Liebmann, B., Fisher, R., Myneni, R.B., 2013. Increased dry-season
629 length over southern Amazonia in recent decades and its implication for future climate
630 projection. *Proceedings of the National Academy of Sciences* 110(45), 18110-
631 18115. <https://doi.org/10.1073/pnas.1302584110>.

632 Gatti, L.V., Domingues, L.G., Basso, L.S., Miller, J.B., Cassol, H.L., Marani, L.,
633 Correia, C.S., Tejada, G., Aragao, L.E.O.C., Anderson, L.O., Gloor, M., Peters, W., Von
634 Randon, C., Neves, R.A.L., Alber, C., Stephane, P., Arai, E., 2021. Sensitivity of Amazon
635 Carbon Balance to climate and human-driven changes in
636 Amazon. <http://repositorio.ipen.br/handle/123456789/32192>.

637 Gessler, A., Ferrio, J.P., Hommel, R., Treydte, K., Werner, R.A., Monson, R.K..
638 2014. Stable isotopes in tree rings: towards a mechanistic understanding of isotope
639 fractionation and mixing processes from the leaves to the wood. *Tree physiology* 34(8),
640 796-818. <https://doi.org/10.1093/treephys/tpu040>.

641 Gloor, M., Brienen, R.J.W., Galbraith, D., Feldpausch, T.R., Schöngart, J., Guyot,
642 J.L., Espinoza, J.C., Lloyd, J., Phillips, O.L., 2013. Intensification of the Amazon
643 hydrological cycle over the last two decades. *Geophys Res Lett* 40, 1729–
644 1733. <https://doi.org/10.1002/grl.50377>.

645 Haghtalab, N., Moore, N., Heerspink, B.P., Hyndman, D.W., 2020. Evaluating
646 spatial patterns in precipitation trends across the Amazon basin driven by land cover and
647 global scale forcings. *Theoretical and Applied Climatology* 140, 411-
648 427. <https://doi.org/10.1007/s00704-019-03085-3>.

649 Heerspink, B.P., Kendall, A.D., Coe, M.T., Hyndman, D.W., 2020. Trends in
650 streamflow, evapotranspiration, and groundwater storage across the Amazon Basin
651 linked to changing precipitation and land cover. *Journal of Hydrology: Regional Studies*
652 32, 100755. <https://doi.org/10.1016/j.ejrh.2020.100755>.

653 Helle, G., Scheleser, G.H., 2004. Beyond CO₂ fixation by Rubisco – an interpretation
654 of ¹³C/¹²C variations in the tree rings from intra-seasonal studies on broad-leaf trees. *Plant*
655 *Cell and Environment* 27: 367-380. <https://doi.org/10.1111/j.0016-8025.2003.01159.x>.

656 Ho, J.T., Thompson, J.R., Brierley, C., 2016. Projections of hydrology in the
657 Tocantins-Araguaia Basin, Brazil: uncertainty assessment using the CMIP5 ensemble.
658 *Hydrological Sciences Journal* 61(3): 551-
659 567. <https://doi.org/10.1080/02626667.2015.1057513>.

660 Holmes, R.L., 1983. Program COFECHA user's manual. Laboratory of Tree-Ring
661 Research, The University of Arizona, Tucson 545-571.

662 IPCC, 2022: Climate Change 2022: Impacts, Adaptation, and Vulnerability.
663 Contribution of Working Group II to the Sixth Assessment Report of the Intergovernmental
664 Panel on Climate Change [H.-O. Pörtner, D.C. Roberts, M. Tignor, E.S. Poloczanska, K.
665 Mintenbeck, A. Alegría, M. Craig, S. Langsdorf, S. Löschke, V. Möller, A. Okem, B. Rama
666 (eds.)]. Cambridge University Press. Cambridge University Press, Cambridge, UK and
667 New York, NY, USA, 3056. <https://doi:10.1017/9781009325844>.

668 Jiménez-Muñoz, J.C., Sobrino, J.A., Mattar, C., Malhi, Y., 2013. Spatial and
669 temporal patterns of the recent warming of the Amazon forest. *Journal of Geophysical*
670 *Research: Atmospheres* 118(11), 5204-5215. <https://doi.org/10.1002/jgrd.50456>.

671 Jiménez-Muñoz, J.C., Mattar, C., Barichivich, J., Santamaría-Artigas, A.,
672 Takahashi, K., Malhi, Y., Sobrino J.A., Schrier, G.V.D., 2016. Record-breaking warming
673 and extreme drought in the Amazon rainforest during the course of El Niño 2015–2016.
674 *Scientific reports* 6(1), 33130.

675 Jiménez-Noriega, M.S., López-Mata, L., Terrazas, T., 2021. Cambial activity and
676 Phenology in three understory species along an altitude gradient in Mexico. *Forests* 12(4):
677 506. <https://doi.org/10.3390/f12040506>.

678 Kagawa, A., Sano, M., Nakatsuka, T., Ikeda, T., Kubo, S., 2015. An optimized
679 method for stable isotope analysis of tree rings by extracting cellulose from cross-

680 sectional laths. Chemical Geology 393, 16-
681 25. <https://doi.org/10.1016/j.chemgeo.2014.11.019>.

682 Kahmen, A., Sachse, D., Arndt, S.K., Tu, K.P., Farrington, H., Vitousek, P.M.,
683 Dawson, T.E., 2011. Cellulose $\delta^{18}\text{O}$ is an index of leaf-to-air vapor pressure difference
684 (VPD) in tropical plants. Proc Natl Acad Sci USA 108: 1981–
685 1986. <https://doi.org/10.1073/pnas.1018906108>.

686 Krottenthaler, S., Pitsch, P., Helle, G., Locosselli, G.M., Ceccantini, G., Altman, J.,
687 Svoboda, M., Dolezal, J., Schleser, G., Anhuf, D., 2015. A power-driven increment borer
688 for sampling high-density tropical wood. Dendrochronologia 36, 40-
689 44. <https://doi.org/10.1016/j.dendro.2015.08.005>.

690 Latrubesse, E., Stevaux, J.C., 2002. Geomorphology and Environmental aspects of
691 Araguaia Fluvial Basin, Brazil. Zeitschrift für Geomorphologie. Supplementband 129:
692 109-127.

693 Li, Z.H., Labbé, N., Driese, S.G., Grissino-Mayer, H.D., 2011 Micro-scale analysis
694 of tree-ring $\delta^{18}\text{O}$ and $\delta^{13}\text{C}$ on α -cellulose spline reveals high-resolution intra-annual
695 climate variability and tropical cyclone activity. Chemical Geology 284(1-2), 138-
696 147. <https://doi.org/10.1016/j.chemgeo.2011.02.015>.

697 Li, Q., Liu, Y., Deng, R., Liu, R., Song, H., Wang, Y., Li, G., 2020. Combination of
698 Tree Rings and Other Paleoclimate Proxies to Explore the East Asian Summer Monsoon
699 and Solar Irradiance Signals: A Case Study on the North China Plain. Atmosphere 11(11),
700 1180. <https://doi.org/10.3390/atmos11111180>.

701 Lisi, C.S., Fo, M.T., Botosso, P.C., Roig, F.A., Maria, V.R., Ferreira-Fedele, L.,
702 Voigt, A.R., 2008. Tree-ring formation, radial increment periodicity, and phenology of tree
703 species from a seasonal semi-deciduous forest in southeast Brazil. Iawa Journal 29(2),
704 189-207. <https://doi.org/10.1163/22941932-90000179>.

705 Liu, Y., Liu, H., Song, H., Li, Q., Burr, G.S., Wang, L., Hu, S., 2017. A monsoon-
706 related 174-year relative humidity record from tree-ring $\delta^{18}\text{O}$ in the Yaoshan region,
707 eastern central China. Sci. Total Environ. 593, 523–
708 534 <https://doi.org/10.1016/j.scitotenv.2017.03.198>.

709 Luchi, A.E., 1998. Periodicidade de crescimento em *Hymenaea courbaril* L. e
710 anatomia ecológica do lenho de espécies de mata ciliar. PhD Thesis, Instituto de
711 Biociências, Universidade de São Paulo.

712 Locosselli, G.M., Buckeridge, M.S., Moreira, M.Z., Ceccantini, G., 2013. A multi-
713 proxy dendroecological analysis of two tropical species (*Hymenaea* spp., Leguminosae)
714 growing in a vegetation mosaic. *Trees* 27, 25-36. <https://doi.org/10.1007/s00468-012-0764-x>.

716 Locosselli, G.M., Schöngart, J., Ceccantini, G., 2016. Climate/growth relations and
717 teleconnections for a *Hymenaea courbaril* (Leguminosae) population inhabiting the dry
718 forest on karst. *Trees* 30, 1127-1136. <https://doi.org/10.1007/s00468-015-1351-8>.

719 Locosselli, G.M., Krottenthaler, S., Pitsch, P., Anhuf, D., Ceccantini, G., 2017. Age
720 and growth rate of congeneric tree species (*Hymenaea* spp.–Leguminosae) Inhabiting
721 different tropical biomes. *Erdkunde* 71, 45-
722 57. <https://doi.org/10.3112/erdkunde.2017.01.03>.

723 Locosselli, G.M., Brienen, R.J., de Souza Martins, V.T., Gloor, E., Boom, A., de
724 Camargo, E.P., Saldiva, P.H.N., Buckeridge, M.S., 2020. Intra-annual oxygen isotopes in
725 the tree rings record precipitation extremes and water reservoir levels in the Metropolitan
726 Area of São Paulo, Brazil. *Science of The Total Environment* 743,
727 140798. <https://doi.org/10.1016/j.scitotenv.2020.140798>.

728 Locosselli, G.M., Miyahara, A.A.L., Cerqueira, P., Buckeridge, M.S., 2021. Climate
729 drivers of tree fall on the streets of São Paulo, Brazil. *Trees* 35, 1807-
730 1815. <https://doi.org/10.1007/s00468-021-02145-4>.

731 Luchi, A.E., 1998. Periodicidade de crescimento em *Hymenaea courbaril* L. e
732 anatomia ecológica do lenho de espécies de mata ciliar. Tese de Doutorado, Instituto de
733 Biociências, Universidade de São Paulo.

734 Maeda, E.E., Ma, X., Wagner, F.H., Kim, H., Oki, T., Eamus, D., Huete, A., 2017.
735 Evapotranspiration seasonality across the Amazon Basin. *Earth System Dynamics* 8(2),
736 439-454. <https://doi.org/10.5194/esd-8-439-2017>, 2017.

737 Malhi, Y., Roberts, J.T., Betts, R.A., Killeen, T.J., Li, W., Nobre, C.A., 2008. Climate
738 change, deforestation, and the fate of the Amazon. *Science* 319(5860), 169-
739 172. <https://doi.org/10.1016/j.ecolind.2021.107798>.

740 Managave, S.R., Sheshshayee, M.S., Borgaonkar, H.P., Ramesh, R., 2010. Past
741 break-monsoon conditions detectable by high resolution intra-annual $\delta^{18}\text{O}$ analysis of
742 teak rings. *Geophysical Research Letters* 37(5), 930-
743 937. <https://doi.org/10.1029/2009GL041172>.

744 Marengo, J.A., 1995. Variations and change in south America streamflow. *Climate*
745 *Change* 31, 99-117. <https://doi.org/10.1007/BF01092983>.

746 Marimon, B.S., Felfili, J.M., Fagg, C.W., Marimon-Junior, B.H., Umetsu, R.K.,
747 Oliveira-Santos, C., Morandi, O.S., Lima, H.S., Nascimento, A.R.T., 2012.
748 Monodominance in a forest of *Brosimum rubescens* Taub. (Moraceae): structure and
749 dynamics of natural regeneration. *Acta oecologica* 43, 134-
750 139. <https://doi.org/10.1016/j.actao.2012.07.001>.

751 Marimon, B.S., Marimon-Junior, B.H., Feldpausch, T.R., Oliveira-Santos, C., Mews,
752 H.A., Lopez-Gonzales, G., Lloyd, J., Franczak, D.D., de Oliveira, E.A., Maracahipes, L.,
753 Miguel, A., Lenza, E., Phillips, O.L., 2014. Disequilibrium and hyperdynamic tree turnover
754 at the forest–cerrado transition zone in southern Amazonia. *Plant Ecology & Diversity* 7,
755 281-292. <https://doi.org/10.1080/17550874.2013.818072>.

756 Marques, E.Q., Marimon-Junior, B.H., Marimon, B.S., Matricardi, E.A., Mews, H.A.,
757 Colli, G.R., 2020. Redefining the Cerrado–Amazonia transition: implications for
758 conservation. *Biodiversity and conservation* 29, 1501-
759 1517. <https://doi.org/10.1007/s10531-019-01720-z>.

760 McCarroll, D., Loader, N.J., 2004. Stable isotopes in tree rings. *Quaternary Science*
761 *Reviews* 23(7-8), 771-801. <https://doi.org/10.1016/j.quascirev.2003.06.017>.

762 Mews, H.A., Marimon, B.S., Maracahipes, L., de Oliveira, E.A., 2012. Temporal
763 analysis of diameter and height distributions in a Semideciduous Seasonal Forest in the
764 Cerrado-Amazon Forest transition, East Mato Grosso, Brazil. *Biotemas* 25(2), 33-43.
765 <https://doi.org/10.5007/2175-7925.2012v25n2p33>.

766 Monson, R.K., Szejner, P., Belmecheri, S., Morino, K.A., Wright, W.E., 2018.
767 Finding the seasons in the tree ring stable isotope ratios. *American Journal of Botany*
768 105(5), 819-821. <https://doi.org/10.1002/ajb2.1083>.

769 Muangsong, C., Pumijumnong, N., Cai, B., Buajan, S., Lei, G., Wang, F., Li, M.,
770 Payomrat, P., 2020. Effect of changes in precipitation amounts and moisture sources on

771 inter-and intra-annual stable oxygen isotope ratios ($\delta^{18}\text{O}$) of teak trees from northern
772 Thailand. *Agricultural and Forest Meteorology* 281,
773 107820. <https://doi.org/10.1016/j.agrformet.2019.107820>.

774 Nobre, P., Malagutti, M., Urbano, D.F., de Almeida, R.A., Giarolla, E., 2009. Amazon
775 deforestation and climate change in a coupled model simulation. *Journal of Climate*,
776 22(21), 5686-5697. <https://doi.org/10.1175/2009JCLI2757.1>.

777 Pagotto, M.A., Menezes, I.R.N., Costa, C.M., Lisi, C.S., Bräuning, A., 2021. Oxygen
778 isotopes in tree rings of *Cedrela odorata* L. as an indicator of hydroclimate variations in a
779 seasonally dry tropical forest in northeastern Brazil. *Trees* 35(6), 1889-
780 1903. <https://doi.org/10.1007/s00468-021-02158-z>.

781 Poussart, P.F., Evans, M.N., Schrag, D.P., 2004. Resolving seasonality in tropical
782 trees: multi-decade, high-resolution oxygen and carbon isotope records from Indonesia
783 and Thailand. *Earth and Planetary Science Letters* 218(3-4), 301-316.

784 Ratter, J., Richards, P.W., Argent, G., Gifford, D.R., 1973. Observations on the
785 vegetation of northeastern Mato Grosso: I - The woody vegetation types of the Xavantina-
786 Cachimbo expedition area. *Philosophical transactions of the Royal Society of London. Series B, Biological sciences* 266(880), 449-489. <https://doi.org/10.1098/rstb.1973.0053>.

788 Richey, J.E., Nobre, C., Deser, C., 1989. Amazon River discharge and climate
789 variability: 1903–1985. *Science* 246(4926), 101–
790 103. <https://doi.org/10.1126/science.246.4926.101>.

791 Risi, C., Bony, S., Vimeux, F., 2008. Influence of convective processes on the
792 isotopic composition ($\delta^{18}\text{O}$ and δD) of precipitation and water vapor in the tropics: 2.
793 Physical interpretation of the amount effect. *Journal of Geophysical Research* 133,
794 D19306. <https://doi.org/10.1029/2008JD009943>.

795 Roden, J.S., Lin, G., Ehleringer, J.R., 2000. A mechanistic model for interpretation
796 of hydrogen and oxygen isotope ratios in tree-ring cellulose. *Geochim. Cosmochim. Acta*
797 64(1), 21–35. [https://doi.org/10.1016/S0016-7037\(99\)00195-7](https://doi.org/10.1016/S0016-7037(99)00195-7).

798 Rosin, C., Amorim, R.S.S., Morais, T.S.T., 2015. Análise de tendências hidrológicas
799 na bacia do rio das Mortes. *Revista Brasileira de Recursos Hídricos* 20(4), 991-998.

800 Salati, E., Dall'Olio, A., Matsui, E., Gat, J.R., 1979. Recycling of water in the Amazon
801 basin: an isotopic study. *Water resources research* 15(5), 1250-1258.
802 <https://doi.org/10.1029/WR015i005p01250>.

803 Santos, G.M., Rodriguez, D.R.O., Barreto, N.O., Assis-Pereira, G., Barbosa, A.C.,
804 Roig, F.A., Tommazello-Filho, M., 2021. Growth assessment of native tree species from
805 Southeastern Brazilian Amazonia by post-AD 1950 ¹⁴C analysis: implications for tropical
806 dendroclimatology studies and atmospheric 14C reconstructions. *Forests* 12(9):
807 1177. <https://doi.org/10.3390/f12091177>.

808 Schollaen, K., Baschek, H., Heirinch, I., Helle, G., 2015. Technical note: an
809 improved guideline for rapid and precise sample preparation of tree-ring stable isotope
810 analysis. *Biogeosciences* 12(14), 11587-11623. [https://doi.org/10.5194/bgd-12-11587-](https://doi.org/10.5194/bgd-12-11587-2015)
811 2015.

812 Schubert, B.A., Timmermann, A., 2015. Reconstruction of seasonal precipitation in
813 Hawai'i using high-resolution carbon isotope measurements across tree rings. *Chemical*
814 *Geology* 417, 273-278. <https://doi.org/10.1016/j.chemgeo.2015.10.013>.

815 Schweingruber, F.H., Eckstein, D., Serre-Bachet, F., Bräker, O.U., 1990.
816 Identification, presentation and interpretation of event years and pointer years in
817 dendrochronology. *Dendrochronologia* 8, 9-38.

818 Steege, H.T., Pitman, N.C., Sabatier, D., Baraloto, C., Salomão, R.P., Guevara, J.
819 E., ..., Silman, M.R., 2013. Hyperdominance in the Amazonian tree flora. *Science*
820 342(6156), 1243092. <https://doi.org/10.1126/science.1243092>.

821 Tiwari, R., Gloor, E., da Cruz, W.J.A., Schwantes Marimon, B., Marimon-Junior, B.
822 H., Reis, S.M., Souza, I.A., Krause, H.G., Slot, M., Winter, K., Ashley, D., Bécu, R.G.,
823 Borges, C.S., da Cunha, M., Fauset, S., Ferreira, L.D.S., Gonçalves, M.D.A., Lopes, T.T.,
824 Marques, E.Q., Mendonça, N.G., Mendonça, N.G., Noletto, P.T., Oliveira, C.H.L., Oliveira,
825 M.A., Pireda, S., Prestes, N.C.C.S., Santos, D.M., Santos, E.B., da Silva, E.L., Souza,
826 I.A., Souza, L.J., Vitória, A.P., Foyer, C.H., Galbraith, D., 2021. Photosynthetic quantum
827 efficiency in south-eastern Amazonian trees may be already affected by climate change.
828 *Plant, Cell & Environment*, 44(7), 2428-2439. <https://doi.org/10.1111/pce.13770>.

829 Vasconcellos, T.J., da Cunha, M., Callado, C.H., 2017. A comparative study of
830 cambium histology of *Ceiba speciosa* (A. St.-Hil.) Ravenna (Malvaceae) under urban

831 pollution. Environmental Science and Pollution Research 24(13), 12049-
832 12062. <https://doi.org/10.1007/s11356-015-6012-3>.

833 Vogado, N.O., de Camargo, M.G.G., Locosselli, G. M., Morellato, L.P.C., 2016.
834 Edge effects on the phenology of the guamirim, *Myrcia guianensis* (Myrtaceae), a cerrado
835 tree, Brazil. Tropical Conservation Science 9(1), 291-
836 312. <https://doi.org/10.1177/194008291600900115>.

837 Vuille, M., Bradley, R.S., Healy, R., Werner, M., Hardy, D.R., Thompson, L.G.,
838 Keimig, F., 2003. Modeling $\delta^{18}\text{O}$ in precipitation over the tropical Americas: 2. Simulation
839 of the stable isotope signal in Andean ice cores. Journal of Geophysical Research:
840 Atmospheres 108(D6). <https://doi.org/10.1029/2001JD002039>.

841 Vuille, M., Werner, M., 2005. Stable isotopes in precipitation recording South
842 American summer monsoon and ENSO variability— Observations and model results.
843 Climate Dynamics 25, 401–413. <https://doi.org/10.1007/s00382-005-0049-9>.

844 Xu, C., Zhu, H., Wang, S.Y.S., Shi, F., An, W., Li, Z., Sano, M., Nakatsuna, T., Guo,
845 Z., 2020. Onset and maturation of Asian summer monsoon precipitation reconstructed
846 from intra-annual tree-ring oxygen isotopes from the southeastern Tibetan Plateau.
847 Quaternary Research 103, 139-147. <https://doi.org/10.1017/qua.2020.28>.

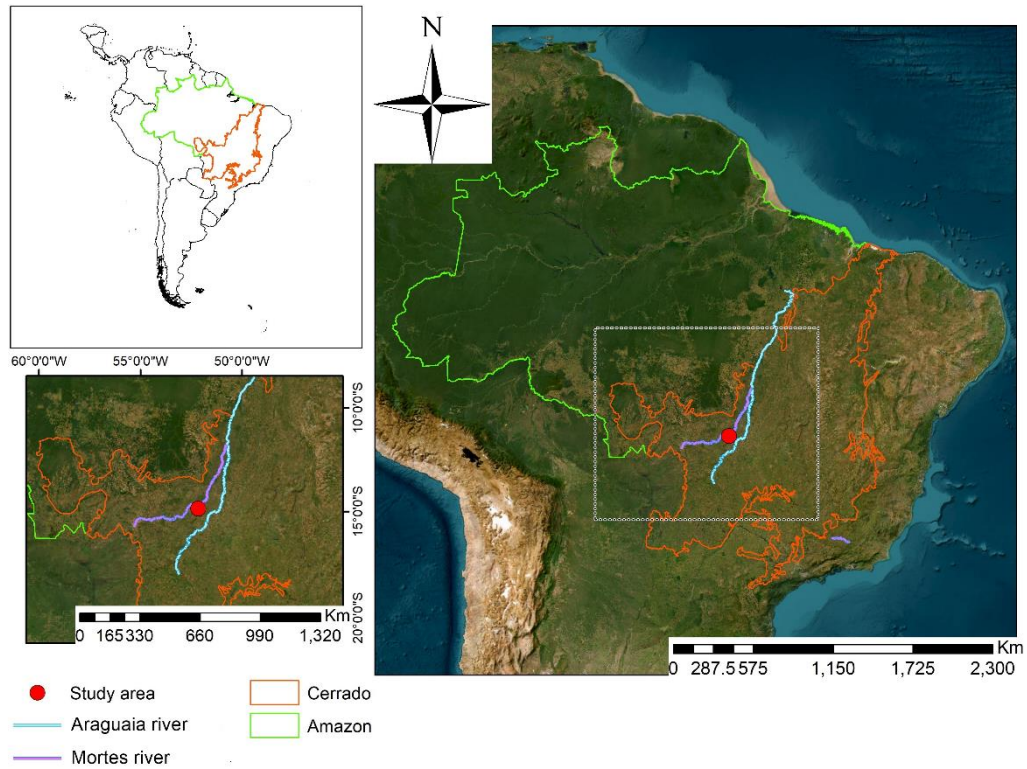
848 Westbrook, J.A., Guilderson, T.P., Colinvaux, P.A., 2006. Annual growth rings in a
849 sample of *Hymenaea courbaril*. Iawa Journal 27(2), 193-197. [https://doi.org/27/2/article-
850 p193_7.xml](https://doi.org/27/2/article-p193_7.xml).

851

852

853

854 **Figures**



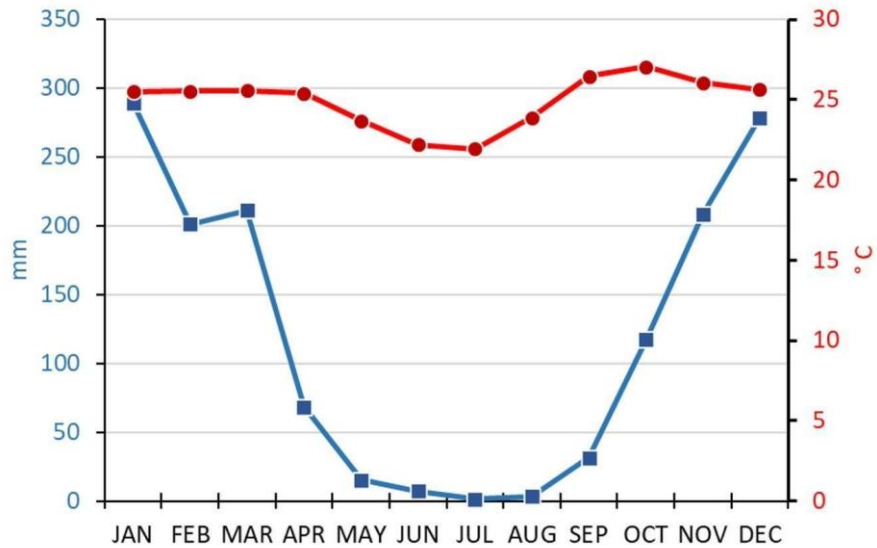
855

856 Figure 1: South America map with the Amazon biome (green line)
 857 and Cerrado biome (red line). The study area (circle) is located at the Amazon forest
 858 fingers, between the Amazonia-Cerrado transition. The main river that drainage the
 859 region is the Araguaia River (blue line) and its main tributary, the Mortes River (purple
 860 line).

861

862

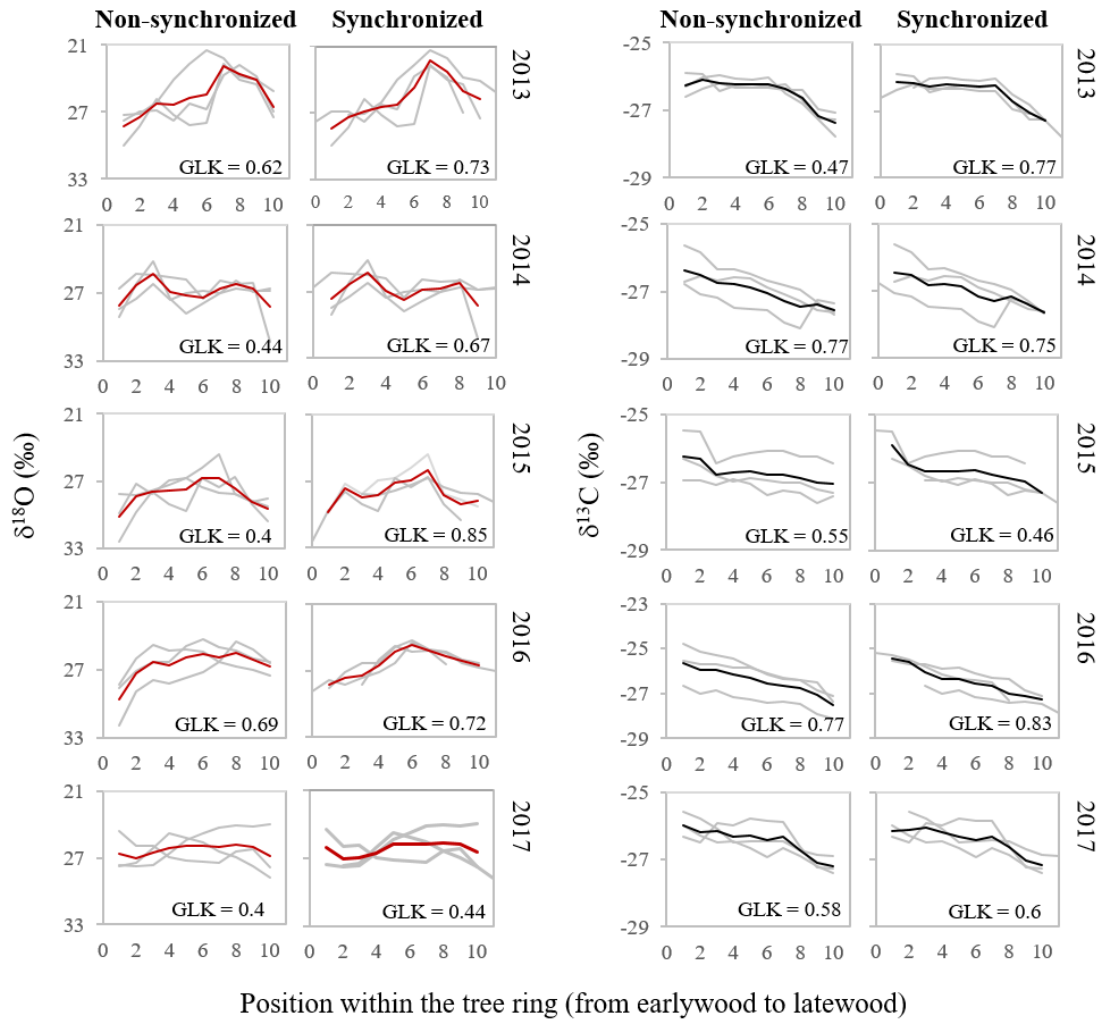
863



864

865 Figure 2: Climate diagram showing temperature and precipitation curves of INMET
 866 (National Institute of Meteorology) data from the Nova Xavantina region between 1998
 867 and 2017. The red line indicates monthly temperature average (°C) and the blue line the
 868 monthly precipitation average (mm), showing a typical tropical climate, with a dry season
 869 between April and September.

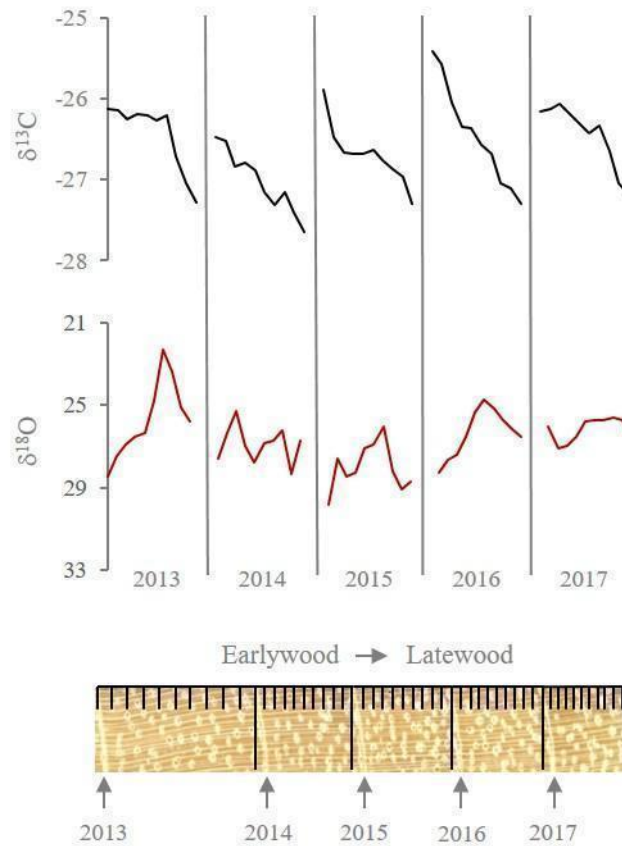
870



871

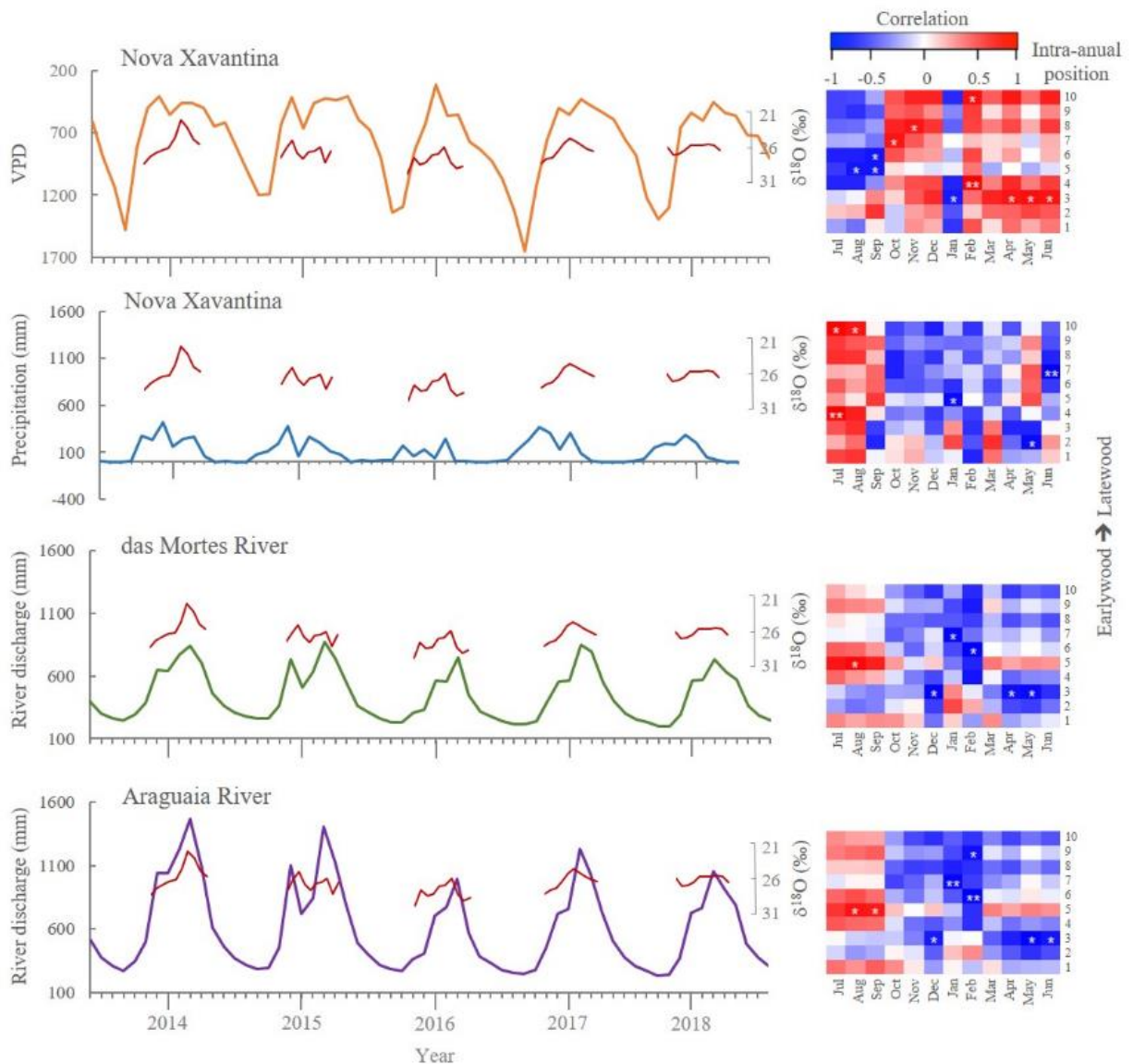
872 Figure 3: Comparisons between non-synchronized and synchronised series of $\delta^{18}\text{O}$
 873 and $\delta^{13}\text{C}$ measured in each tree ring of *Hymenaea courbaril* trees samples from the
 874 southern Amazon. Series of individual trees are represented in grey, while the average
 875 series of $\delta^{18}\text{O}$ is represented in red and $\delta^{13}\text{C}$ in black. GLK averages were calculated for
 876 all positions. The y-axis for the $\delta^{18}\text{O}$ series are reversed.

877



878

879 Figure 4: Average of annual $\delta^{13}\text{C}$ and $\delta^{18}\text{O}$ synchronised series between 2013 and
 880 2017, positioned from earlywood (position 1) to latewood (position 10). The y-axis for the
 881 $\delta^{18}\text{O}$ are reversed. Above a sampled radius of *Hymenaea courbaril* as an example of the
 882 10 divisions made in each tree ring. Separations were performed by dividing the weight
 883 of the tree ring into ten parts.

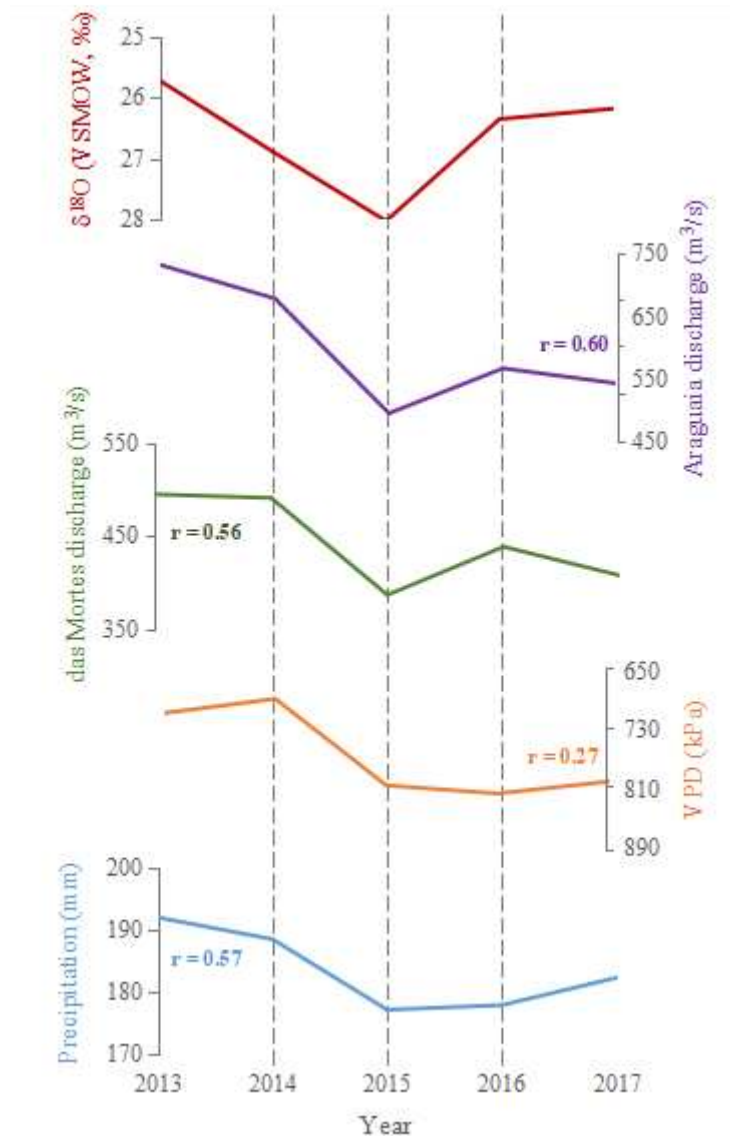


884

885 Figure 5: Vapour Pressure Deficit (orange line), Precipitation (blue line),
 886 Mortes (green line), and Araguaia river discharge (purple line) between June 2013 and
 887 July 2018. The mean oxygen isotopic series (red lines) were positioned according to the
 888 best correlation found between monthly climate data and the isotopic positions within the
 889 tree rings (oxygen isotope at position 5 within the tree ring aligned in January). For the
 890 relationship with the rivers, we took into account the gap of approximately 1 month
 891 between the beginning of the rainy season and the increase in river flow (oxygen isotope
 892 at position 5 within the tree ring aligned in February). The y-axes for $\delta^{18}\text{O}$ and VPD have
 893 been reversed solely for visual comparison purposes and not for statistical analysis.
 894 Heatmaps show the correlation values between oxygen isotopic series and climate data.
 895 For the intra-annual position the sample sizes are $n = 5$. Correlation values are presented
 896 per month between vapour pressure deficit, precipitation, and river discharges. *

897 significant values for $\alpha = 0.05$ and ** for $\alpha = 0.01$. Climate data were obtained from climate
898 stations of the cities of Nova Xavantina and Cocalinho, Mato Grosso, Brazil.

899



900

901 Figure 6: Annual oxygen isotope series of *Hymenaea courbaril* (red line), local
902 precipitation (blue line), Araguaia river discharge (purple line), das Mortes river discharge
903 (green line), and Vapour Pressure Deficit (orange line) between 2013 and 2017. The
904 annual isotope series correspond to the average of the 3 to 7 ($n = 5$ samples for each
905 position) isotope positions within the tree ring and the hydroclimatic data comprise the
906 rainy season average, from October to March. Values indicate the Pearson correlation
907 coefficients between the $\delta^{18}\text{O}$ and the records for the period shown (for all $P < 0.001$).

908 Note that the y-axis for the $\delta^{18}\text{O}$ and VPD are reversed for visual comparison purposes
909 but not for statistical analysis.